Photoelectron spectroscopy of sulfur atoms produced via twophoton dissociation of sulfur dioxide

J. R. Appling, M. R. Harbol, R. A. Edgington, and A. C. Goren

Citation: The Journal of Chemical Physics **97**, 4041 (1992); doi: 10.1063/1.463933
View online: http://dx.doi.org/10.1063/1.463933
View Table of Contents: http://scitation.aip.org/content/aip/journal/jcp/97/6?ver=pdfcov
Published by the AIP Publishing

Photoelectron spectroscopy of sulfur atoms produced via two-photon dissociation of sulfur dioxide

J. R. Appling,[a] M. R. Harbol, and R. A. Edgington
Department of Chemistry, University of Kentucky, Lexington, Kentucky 40506

A. C. Goren
Department of Chemistry, Transylvania University, Lexington, Kentucky 40508

(Received 13 April 1992; accepted 27 May 1992)

The 2+1 resonantly enhanced multiphoton ionization (REMPI) spectrum of sulfur atoms produced by two-photon photodissociation of sulfur dioxide is reported for the wavelength range 252–263 nm. Photoelectron spectroscopy of many resonant ionizations reveals a propensity toward preservation of ion core configuration in formation of ionic species. Several pathways for production of pure populations of excited state $^2D^o_J$ sulfur ions are documented. Photoelectron angular distributions show contributions from outgoing electrons with a maximum angular momentum $l_{max}=2$. Intermediate state alignment from two-photon absorption of ground state $^3P_0$ sulfur atoms is demonstrated.

I. INTRODUCTION

The spectroscopy and photochemistry of sulfur-containing molecules have received much attention over the past decade. Atomic sulfur is of fundamental interest in chemistry and physics with regard to spectroscopy and dynamics of heavier, open-shell atoms. It is also of atmospheric and industrial interest because it is oxidized rapidly and thus becomes a contributor toward the formation of acid rain.[1] Our interest in sulfur-containing molecules stems from their ability to yield ground and excited state sulfur atoms upon photodissociation using ultraviolet laser radiation. Because of its energy level structure, sulfur is a good candidate for creation of state-selected ions. Using resonantly enhanced multiphoton ionization (REMPI) coupled with photoelectron spectroscopy (PES), we have determined several propensities for ionic state formation through ionization pathways which will yield state-selected sulfur ions for future ion–molecule investigations. We present here the 2+1 REMPI-PES and photoelectron angular distributions of atomic sulfur arising from two-photon photodissociation of SO_2 in the wavelength region 252–263 nm.

Atomic sulfur is produced easily by photodissociation of a sulfur-containing parent molecule such as SO_2,[2–4] CS_2,[5–7] OCS,[8,9] or H_2S.[10] In this study, sulfur dioxide was dissociated by a two-photon absorption of ultraviolet light. In the 252–263 nm wavelength region, SO_2 undergoes a two-photon absorption through the $\tilde{G}$ state followed by dissociation[2–4] according to the following scheme:

$$SO_2(\tilde{X}\,^1A_1) \rightarrow SO_2(\tilde{A},\tilde{B}) \rightarrow SO_2(\tilde{G}) \begin{cases} \nearrow S(^3P,^1D,^1S)+O_2(X\,^3\Sigma_g^-, a\,^1\Delta_g) \\ \searrow SO(X\,^3\Sigma^-,\ a\,^1\Delta,\ b\,^1\Sigma^+)+O(^3P,^1D). \end{cases}$$

The ground state configuration of neutral sulfur[11] is $1s^22s^22p^63s^23p^4$, which splits into three terms ^3P, ^1D, and ^1S, in order of increasing energy. It has been shown that sulfur can be produced in all three levels[5] depending on the identity of the parent molecule as well as the wavelength of laser light used in the photodissociation. The ground state configuration of ionic sulfur is $1s^22s^22p^63s^23p^3$ which splits into three terms $^4S^o$, $^2D^o$, and $^2P_0$, also in order of increasing energy. An energy level diagram for the $S(I)$–$S(II)$ system is shown in Fig. 1.

Resonantly enhanced multiphoton ionization can be an effective technique for producing state-selected ions, which in turn can be used as participants in ion–molecule reactions.[12,13] Photoelectron detection coupled with REMPI yields valuable information concerning the final states of the ionic species, as well as facilitating assignments of the intermediate neutral states accessed in the $n+m$ REMPI transition. While several groups have studied S^+ fragments by MPI,[5,6,8,10] few[10] have characterized the ionization dynamics with photoelectron spectroscopy. Our REMPI-PES measurements between 252 and 263 nm permit the assignment of two-photon resonances and final ion states. Although both ^3P_J and $^1D_2$ sulfur atoms are expected to be formed in the SO_2 dissociation, the $^1D_2$ atoms cannot be probed using 2+1 REMPI in this wavelength region.[11]

Photoelectron angular distribution measurements allow the characterization of aligned atomic states. In this

[a]Author for correspondence. Present address: Department of Chemistry, Clemson University, Clemson, SC 29634.

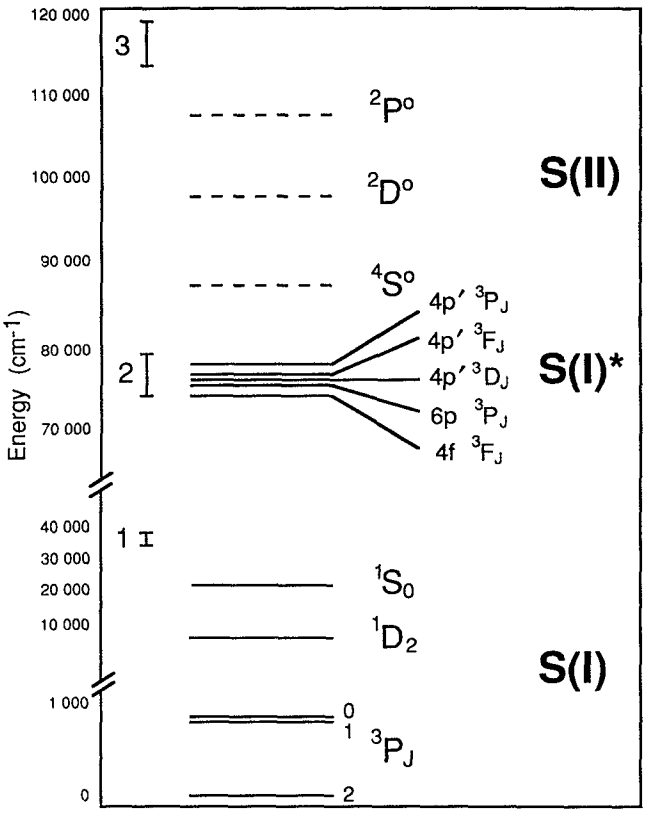

FIG. 1. A schematic energy-level diagram of the relevant states of S and S^+. Note breaks in the energy axis. Vertical bars indicate the one-, two-, and three-photon levels, respectively, accessed in the present study.

study, we document optical alignment of $^3P_0$ sulfur atoms ionized via 2+1 REMPI pathways. Ground state $^3P_1$ and $^3P_2$ sulfur atoms can be aligned by the photodissociation process itself; however, the single-color experiments described here cannot detail this alignment quantitatively. The photoelectron angular distributions observed are interesting nonetheless and will provide direction for future two-color laser experiments on this system.

The angular distribution of photoelectrons created by an $(n+1)$ REMPI process utilizing a single, linearly polarized laser follows the form[14–18]

$$W_e(\Theta)\alpha \sum_{k=0}^{k_{max}} a_{2k}P_{2k}(\cos\Theta). \quad (1)$$

The $P_{2k}(\cos\Theta)$ terms are Legendre polynomials of order $2k$ and Θ is the angle between the light polarization and photoelectron propagation vectors. The a_{2k} coefficients contain information about the partial wave character of the outgoing electron and alignment of the intermediate resonant state.[17] For spherically symmetric excited states such as $^3P_0$ states accessed in the present study, expression (1) reduces to $a_0+a_2P_2(\cos\Theta)$. The ratio $A_2=a_2/a_0$ parallels the familiar asymmetry parameter β used in conventional description of single-photon ionization.[19–21] Higher order terms $(k>1)$ may be prominent in description of ionization from aligned resonant intermediate states.

In an $(n+1)$ REMPI process, k is limited to $k_{max}=n+1$, which dictates that the highest-order Legendre polynomial predicted for fits to our 2+1 REMPI-PES photoelectron angular distributions would be $P_6(\cos\Theta)$. However, angular momentum constraints can reduce k_{max}. In fact, all our measured angular distributions were fit with either A_2 coefficients alone, or a combination of A_2 and A_4 coefficients. For $(n+1)$ REMPI via one intermediate J' level, k_{max} will be the smaller of $n+1$, $J'+1$, or l_{max}.[17,18,22] Thus angular distribution measurements can provide information on l_{max}, the maximum orbital angular momentum of the ejected electron.

II. EXPERIMENT

The experiments reported here consist of four separate types of measurements—time-of-flight (TOF) mass spectra, wavelength spectra for S^+ production, TOF photoelectron spectra, and photoelectron angular distributions. All experiments were performed using the same photoion/photoelectron spectrometer. The interaction region and flight tube are shown schematically in Fig. 2, along with a diagram of the optical train and electronic connections.

The spectrometer construction is based on a 6 in. stainless steel vacuum tee with additional ports for laser windows and an extension which houses the flight tube. The spectrometer sits above a pumping stack consisting of a pneumatic gate valve (Vacuum Research Co.), a freon-cooled Chevron baffle (CRC), and a 2200 L/s diffusion pump (Varian VHS-6) backed by a 23 cfm roughing pump (Sargent–Welch 1374). A background pressure of 2×10^{-7} Torr is maintained in the absence of sample gases. Sample gases are admitted into the interaction region through a 70 μm orifice in a molybdenum disk (Ted Pella, Inc.) which has been attached to a copper repeller plate. The repeller plate is electrically isolated and positioned opposite to the opening of the flight tube and parallel to the laser propagation axis. Sample gas is delivered to a fitting on the back of the repeller plate via 1/8 in. diameter Tefzel tubing. A micrometer valve is used to adjust the backing pressure of sample gas to establish an approximate chamber pressure of 1×10^{-5} Torr for experimental measurements.

The flight tube consists of an aluminum cylinder capped with an aluminum face plate. This face plate may be fitted with copper disks which have openings of various sizes. An opening of 2 mm was used for these studies. This geometry yields an acceptance angle of 4.5°, which fills the 40 mm channel plate detector at a flight distance of approximately 50 cm. The flight tube contains a copper mesh Faraday cage which was grounded for both ion and photoelectron studies. In order to reduce the effect of ambient magnetic fields on photoelectron trajectories, a set of dual matched magnetic shields (Ad Vance Magnetics) surrounds the flight tube and the interaction region. A modified Comstock CP-602 dual microchannel plate allows detection of both ions and electrons, depending on the bias and configuration of the high voltage electronics. A grounded, 90% transmittance nickel grid was attached in front of the first microchannel plate to ensure field-free

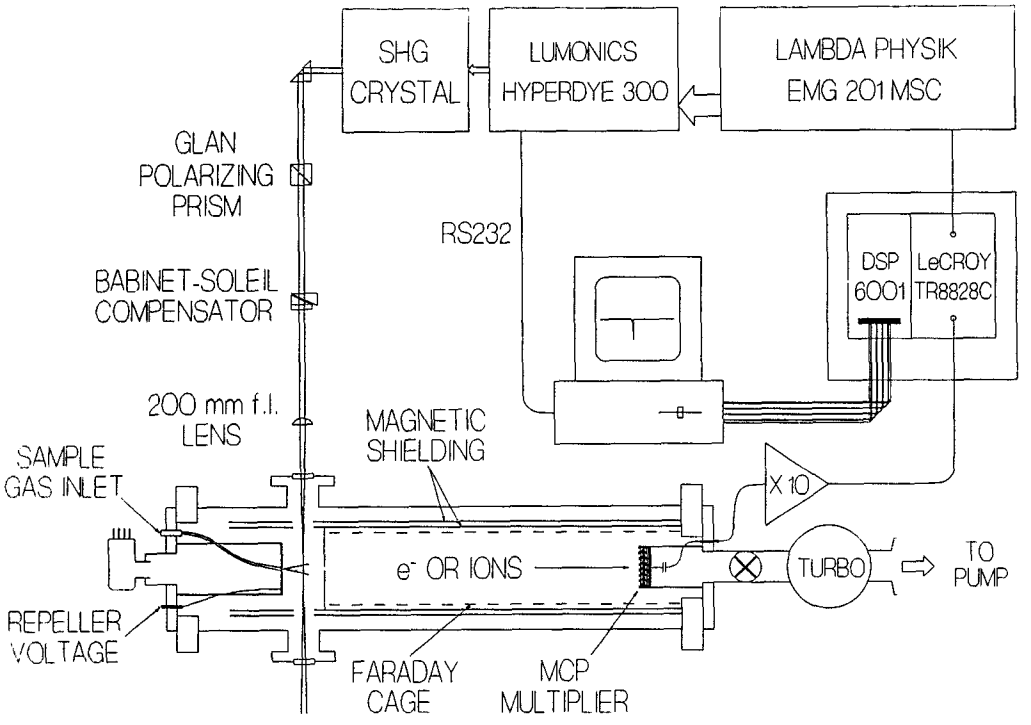

FIG. 2. A schematic diagram of the experimental design.

behavior of photoelectrons. The flight tube is pumped differentially by a 50 L/s turbomolecular pump (Balzers).

The signal from the detector is preamplified (Ortec 9301) before being digitized by a LeCroy TR8828C 200 MHz transient recorder. The digitizer is interfaced to a microcomputer (PC's limited 12 MHz AT clone) with a DSP 6001 computer-aided measurement and control (CAMAC) crate controller. A trigger is provided by the firing circuit of the excimer pump laser, distributed to the digitizer and other NIM units through a BNC 8010 signal generator. Also resident in the CAMAC crate (Kinetic Systems 1502) is a stepping motor controller (Kinetic Systems 3362) for manipulation of a rotation stage supporting the Babinet–Soleil compensator. All data acquisition and control of CAMAC units is through custom software written in Turbo Pascal (Borland International, Inc.).

A Lambda Physik EMG 201 MSC excimer laser operated at 308 nm (XeCl) was used to pump a Lumonics Hyperdye 300 dye laser. All experiments reported here were performed using Coumarin 500 laser dye (Exciton) in methanol. Output of the dye laser entered a Lumonics Hypertrak 1000 for frequency doubling with a BBO crystal. Control of wavelength and crystal tuning curves was provided through interface of the Lumonics control unit to our computer via RS232 communication. Polarization purity of the ultraviolet laser beam was maintained with a Glan polarizing prism (Karl Lambrecht). The laser beam entered the vacuum chamber after passing through a 200 mm focal length fused silica lens. Control of focal point was provided in three dimensions with *XYZ* positioners (Ealing).

Photoelectron angular distributions were measured by fixing the wavelength of the laser to correspond to the resonance of interest and recording photoelectron intensity as a function of the angle made between the laser polarization axis and the TOF axis. The polarization was manipulated using a Babinet–Soleil compensator (Karl Lambrecht) that had been tuned for half-wave retardation for each wavelength investigated. The compensator was mounted on a rotation stage controlled via software.

For an angular distribution measurement, the compensator was rotated through 180° and reversed at 10° intervals. Forty laser shots were summed at each interval and each angular distribution was a histogram of 20 such cycles. Thus each data point was the sum of photoelectron intensity compiled for 800 laser shots. Photoelectron angular distribution data were normalized and fit to expression (1) using a Legendre polynomial fit in the math transform feature of SigmaPlot 4.0 (Jandel Scientific).

III. RESULTS

Multiphoton ionization of SO_2 in the range 252–263 nm yields the ionic fragments S^+ and SO^+ exclusively. No parent SO_2^+ or O^+ fragment ions are observed. This is consistent with earlier MPI investigations by Asscher *et al.*[23] A portion of the REMPI spectrum of atomic sulfur (S^+ ions vs laser wavelength) is shown in Fig. 3 for the wavelength region 254–259 nm. Ion intensities were not corrected for fluctuations in laser power. The sharp features in the spectrum indicate atomic transitions of sulfur atoms released from the photodissociation of SO_2 by the same laser pulse which probes the sulfur atom transition. Most of the observed resonances are due to 2+1 multipho-

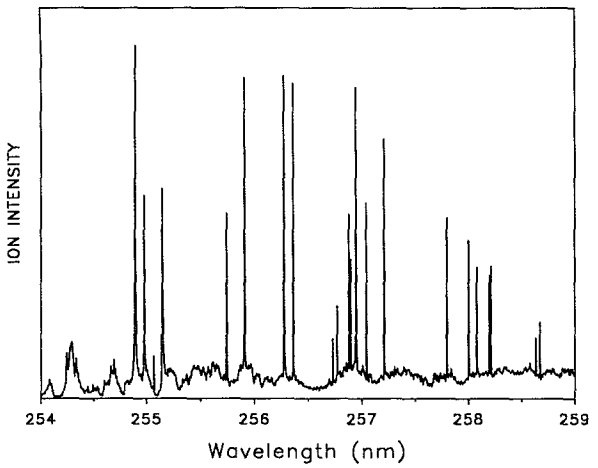

FIG. 3. A portion of the 2+1 REMPI spectrum of *S* from the photodissociation of SO_2.

ton ionization of atomic sulfur produced in the two-photon dissociation of SO_2. Investigation of SO^+ ion intensity as a function of laser wavelength yields spectra with pronounced dips at wavelengths that correspond to the 2+1 REMPI transitions of sulfur atoms. These dips are caused by ion–electron recombination which occurs in the interaction region before SO^+ ions are extracted and sent along the flight tube axis.

Analysis of our sulfur MPI data followed from simple subtraction of two-photon transition energies while looking for members of various series such as $^3F_J \leftarrow\leftarrow {}^3P_2$ or $^3D_2 \leftarrow\leftarrow {}^3P_J$. This method of analysis was also used to determine the wavelength calibration of our laser. We were able to make logical assignments for 25 observed lines after converting the raw wavelength data using a polynomial fit (SigmaPlot 4.0) to match literature values.[11] This "internal" calibration was further substantiated independently by calibration of the laser to neon transitions measured using a neon-filled hollow cathode lamp. Our measured two-photon energies agreed to within a few wavenumbers of those tabulated for sulfur,[11] as shown in Table I. Subsequent analysis of photoelectron data helped to substantiate our initial assignments.

Representative photoelectron spectra are shown in Fig. 4. The resolution of our spectrometer is sufficient to separate electron peaks arising from formation of ground, first, and second excited states of sulfur ions. We were unable to resolve electron energy peaks due to *J* splitting in $^2D^o_{5/2,3/2}$ or $^2P^o_{3/2,1/2}$ ion states which are separated by 31.8 cm^{-1} (3.9 meV) and 46.7 cm^{-1} (5.8 meV), respectively.

The raw PES data consist of electron time-of-flight distributions summed from 500 laser shots. These data were converted to electron energies after calibrating the time axis in a separate experiment using literature values[24] for 3+1 REMPI transitions of xenon. The measured electron energies in the PES experiments yield information concerning final ion states. Thus, branching ratios for ionization can be determined. Since peak widths of fast photoelectrons were comparable to the response time of our detection electronics, peak heights have been used to represent these ratios. The PES data are summarized in Table II.

TABLE I. Assignments of observed (2+1) REMPI of ground state atomic sulfur.

Wavelength (nm)	Initial state	2 $h\nu$ (cm^{-1})	2 $h\nu+E_0$[a] (cm^{-1})	Energy[b] (cm^{-1})	Excited state
253.132	$^3P_1$	79 010	79 406	79 405	$(^2D)4p'\ ^3P_1$
253.662	$^3P_0$	78 845	79 419	79 418	$(^2D)4p'\ ^3P_0$
254.893	$^3P_2$	78 464	78 464	78 463	$(^2D)4p'\ ^3F_4$
254.984	$^3P_2$	78 436	78 436	78 436	$(^2D)4p'\ ^3F_3$
255.069	$^3P_2$	78 410	78 410	78 410	$(^2D)4p'\ ^3F_2$
255.150	$^1D_2$	78 385	87 624	[c]	$(^2D)5p\ ^1P_1$
255.744	$^3P_2$	78 203	78 203	78 203	$(^2D)4p'\ ^3D_3$
255.908	$^3P_2$	78 153	78 153	78 152	$(^2D)4p'\ ^3D_{2,1}$
256.278	$^3P_1$	78 040	78 436	78 436	$(^2D)4p'\ ^3F_3$
256.364	$^3P_1$	78 014	78 410	78 410	$(^2D)4p'\ ^3F_2$
256.741	$^3P_2$	77 900	77 900	77 902	$(^4S)6p\ ^3P_0$
256.769	$^3P_2$	77 891	77 891	77 891	$(^4S)6p\ ^3P_2$
256.894	$^3P_2$	77 853	77 853	77 855	$(^2D)6p\ ^1P_1$
256.908	$^3P_2$	77 849	77 849	77 851	$(^4S)6p\ ^5P_1$
256.950	$^3P_0$	77 836	78 410	78 410	$(^2D)4p'\ ^3F_2$
257.056	$^3P_1$	77 804	78 200	78 203	$(^2D)4p'\ ^3D_3$
257.214	$^3P_1$	77 756	78 152	78 152	$(^2D)4p'\ ^3D_{2,1}$
257.801	$^3P_0$	77 579	78 153	78 152	$(^2D)4p'\ ^3D_{2,1}$
258.004	$^3P_1$	77 518	77 914	77 914	$(^4S)6p\ ^3P_1$
258.094	$^3P_1$	77 491	77 887	77 891	$(^4S)6p\ ^3P_2$
258.211	$^3P_1$	77 456	77 852	77 855	$(^2D)4p'\ ^1P_1$
258.227	$^3P_1$	77 451	77 847	77 851	$(^4S)6p\ ^5P_1$
258.649	$^3P_0$	77 325	77 899	77 902	$(^4S)6p\ ^3P_0$
258.685	$^3P_0$	77 314	77 888	77 891	$(^4S)6p\ ^3P_2$
260.909	$^3P_2$	76 655	76 655	76 656	$(^4S)4f\ ^3F_{4,3,2}$
262.273	$^3P_1$	76 256	76 653	76 656	$(^4S)4f\ ^3F_{3,2}$
262.872	$^3P_0$	76 083	76 656	76 656	$(^4S)4f\ ^3F_2$

[a]Two-photon excited intermediate state energy calculated by adding the two-photon energy and the energy of the initial state with respect to the ground state, $^3P_2$ (Ref. 11).
[b]Excited intermediate state energies (Ref. 11).
[c]Autoionizing level reported by Appling, *et al.* (Ref. 26).

A summary of photoelectron angular distributions is presented in Table III for photoelectron energies that were easily measured. The fitted coefficients A_2 and A_4 from expression (1) are listed for transitions grouped by initial sulfur atomic state. A typical photoelectron angular distribution is presented in Fig. 5. This 2+1 REMPI transition originates in the $^3P_0$ ground state and resonantly accesses the $4p'\ ^3P_0$ intermediate state, neither of which can be aligned. As expected, the best fit to this angular distribution employs the second Legendre term only, with $A_2 = 1.36$. In contrast to this $P_2(\cos\Theta)$ behavior, the angular distribution shown in Fig. 6 must be fit with the next higher term in the expansion of Eq. (1). This distribution is also different in that it is peaked at 45°, as are only two others in Table III. All remaining angular distributions are peaked at 0° along the flight tube axis.

The data depicted in Figs. 5 and 6, and listed in Table III, were normalized to unity. Normalized data were used for all fits and there was no additional data smoothing employed. As can be seen in the figures, the quality of data is very good and reproducibility suggests error in A_2 of approximately ±0.05. However, the $4p'\ ^3F_3 \leftarrow\leftarrow {}^3P_1$ tran-

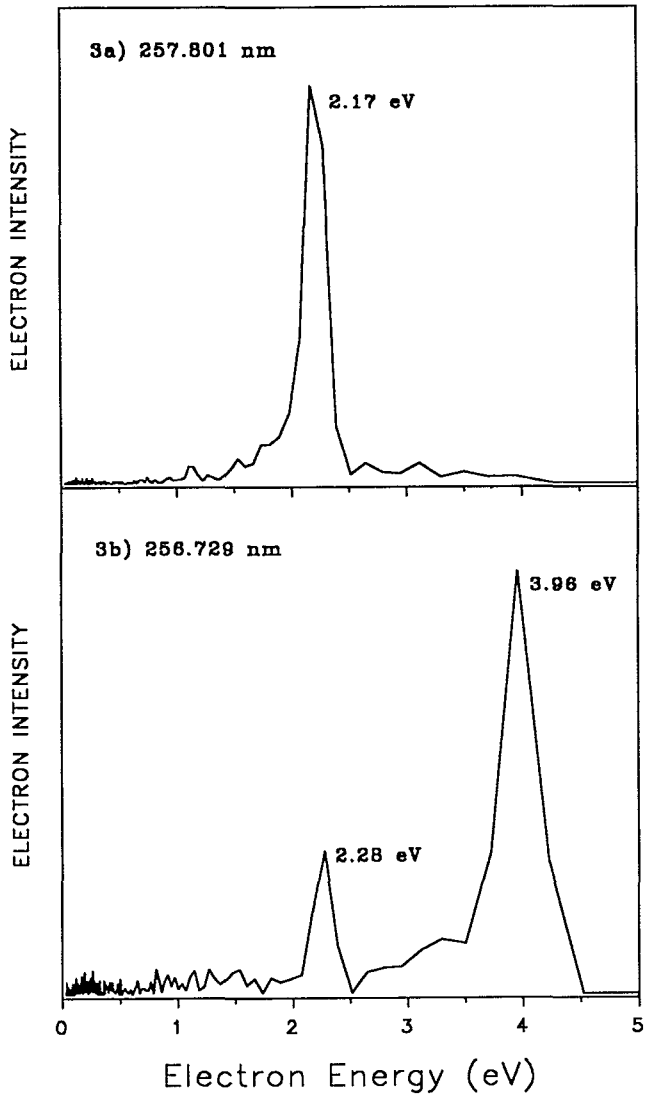

FIG. 4. Representative REMPI-PES spectra.

sition yields a value of $A_2=2.10$, clearly above the theoretical maximum[25] of 2. Thus we increase our estimate of the uncertainty in A_2 to ± 0.1. The data for ionization of atoms through $^3P_0$ intermediate states gives a check on the error in A_4. Transitions of this type must yield photoelectron angular distributions fit by A_2 only; all higher orders must be equal to zero. Values for A_4 can range between -1 and $+7/3$, and we observe values from -0.87 to $+0.93$. Fits to the observed $6p\ ^3P_0 \leftarrow\leftarrow {}^3P_2$ transitions (symmetric intermediate state) suggest an error of ± 0.15 in A_4 coefficients. The magnitudes of these errors in A_2 and A_4 were unexpected since they are larger than statistical errors determined for the fits.

IV. DISCUSSION

A. REMPI of atomic sulfur

Referring to Table I, we note that all 2+1 REMPI transitions occur from the sulfur ^3P_J ground state. Although we observe $^1D_2$ state sulfur atoms produced from SO_2 photodissociation, we are unable to probe these atoms by 2+1 or 1+1 REMPI in this wavelength region. However, it is possible to access autoionizing levels via two-photon absorptions from the $^1D_2$ state. Indeed, we were able to assign a new autoionizing level using our PES results. We have discussed this observation previously[26] in a publication detailing state-selective charge exchange reactions of S^+ ions with OCS.

Symmetry rules permit the correlation of atomic states in two-photon absorption with linearly polarized light according to the following selection rules: $\Delta S=0$; $\Delta J=0, \pm 1, \pm 2$ with $J=0 \nleftrightarrow J=1$; $\Delta L=0, \pm 1, \pm 2$ with $L=0 \nleftrightarrow L=1$ (Ref. 6); and $\Delta l=0, \pm 2$.[5,10] Thus, we observe intense $np \leftarrow\leftarrow 3p$ as well as weak $4f \leftarrow\leftarrow 3p$ transitions. It is uncertain at the present time whether the $4f \leftarrow\leftarrow 3p$ transitions are weaker because $\Delta l=+2$ is less favored or because these transitions occur in a low power portion of the dye curve. None of the forbidden $nd \leftarrow\leftarrow 3p$ or $ns \leftarrow\leftarrow 3p$ transitions were observed.

Most of the observed two-photon transitions adhere strictly to Russell–Saunders (L–S) coupling rules, indicating that the sulfur energy states involved can be described by the spin–orbit coupling scheme. However, transitions at 256.894, 256.908, 258.211, and 258.227 nm violate the conservation of electron spin. Similar types of violations were noted by Steadman and Baer[10] and Venkitachalam and Rao[5] in sulfur studies in the 288–310 nm region. Jackobsson,[27] in an IR emission study of a high frequency SO_2 discharge, noted substantial configuration interaction between the $6p\ ^3P_1$, $6p\ ^5P_1$, and $4p'\ ^1P_1$ levels of atomic sulfur explaining observed singlet–quintet transitions.

B. Photoelectron spectroscopy

Conventional photoionization involves the removal of a single electron from the neutral species without changing the quantum numbers of any other electrons. For an atom, if the angular momentum of the original electron is designated l then the change in L between the neutral species and the ion is given by

$$\Delta L=0, \pm 1, \ldots, \pm l$$

and the rule for change in spin multiplicity becomes

$$\Delta S=\pm 1.$$

Since ionizations in our experiment occur with the absorption of one photon from an intermediate state, we can view these processes in terms of this conventional photoionization.

A comparison can be made between calculated photoelectron energies expected, according to the rules for photoionization stated above, and measured electron energies. This information is given in Table II. The number in parentheses indicates the observed branching ratios measured with the laser polarization along the TOF axis. We have successfully assigned final ion states without violation of selection rules for ionization. Note that due to low laser power in this wavelength region of the laser dye, electron signals from the $4f\ ^3F_J$ intermediate state were too weak to assign reliably. The appearance of intercombination tran-

TABLE II. Observed (2+1) REMPI-PES of atomic sulfur.

Wavelength (nm)	Initial state	Intermediate state	Ion states[a] $^4S^o$	$^2D^o$	$^2P^o$
253.132	$^3P_1$	$4p'\,^3P_1$	4.38 (18)	2.54 (82)	1.34(0)
253.662	$^3P_0$	$4p'\,^3P_0$	4.37 (19)	2.53 (81)	1.33(0)
254.893	$^3P_2$	$4p'\,^3F_4$		2.39(100)	
254.980	$^3P_2$	$4p'\,^3F_3$		2.39(100)	
255.069	$^3P_2$	$4p'\,^3F_2$		2.38(100)	
255.150	$^1D_2$	$5p\,^1P_1$	0.54[b](100)		
255.744	$^3P_2$	$4p'\,^3D_3$		2.34(100)	1.14(0)
255.908	$^3P_2$	$4p'\,^3D_{2,1}$		2.33(100)	1.13(0)
256.278	$^3P_1$	$4p'\,^3F_3$		2.36(100)	
256.364	$^3P_1$	$4p'\,^3F_2$		2.36(100)	
256.741	$^3P_2$	$6p\,^3P_0$	4.13 (74)	2.29 (26)	1.09(0)
256.769	$^3P_2$	$6p\,^3P_2$	4.20 (42)	2.36 (50)	1.16(8)
256.894	$^3P_2$	$4p'\,^1P_1$	4.12	2.28	1.08
256.908	$^3P_2$	$6p\,^5P_1$	4.12	2.28	1.08
256.950	$^3P_0$	$4p'\,^3F_2$		2.35(100)	
257.056	$^3P_1$	$4p'\,^3D_3$		2.32(100)	1.12(0)
257.214	$^3P_1$	$4p'\,^3D_{2,1}$		2.31(100)	1.11(0)
257.801	$^3P_0$	$4p'\,^3D_{2,1}$		2.30(100)	1.10(0)
258.004	$^3P_1$	$6p\,^3P_1$	4.10	2.27(100)	1.07(0)
258.094	$^3P_1$	$6p\,^3P_2$	4.10 (75)	2.26 (25)	1.06(0)
258.211	$^3P_1$	$4p'\,^1P_1$	4.09	2.25	1.05
258.227	$^3P_1$	$6p\,^5P_1$	4.09	2.25	1.05
258.649	$^3P_0$	$6p\,^3P_0$	4.09 (75)	2.25 (25)	1.05(0)
258.685	$^3P_0$	$6p\,^3P_2$	4.09 (78)	2.25 (22)	1.05(0)
260.909	$^3P_2$	$4f\,^3F_{4,3,2}$	3.90	2.05	0.86
262.273	$^3P_1$	$4f\,^3F_{3,2}$	3.87	2.03	0.83
262.872	$^3P_0$	$4f\,^3F_2$	3.86	2.02	0.82

[a]Calculated photoelectron energies in electron volts. Numbers in parentheses indicate observed branching ratios along the laser polarization axis. Data without branching ratios indicate that the transition was too weak to measure electron energies accurately.
[b]$S^+(^4S^o)$ produced by two-photon autoionization from $S\,^1D_2$ (Ref. 26).

sitions was weak and dependent on laser power, so those electron energies were also too weak to assign. The final ion state dynamics should be examined by not only applying the simple rules for ionization, but also by studying how the ion core of the intermediate state is preserved or changed in the ionization process. This is discussed in the next section.

C. Ionization from intermediate states

The REMPI-PES data tabulated in Table II can be grouped according to excited intermediate states. In this way, we observe similarities in ionization among certain transitions.

(1) $(^2D^o)4p'\,^3F_J$. Ionization through $4p'\,^3F_J$ resonant states produces only $^2D^o$ sulfur ions. The $4p'\,^3F_J$ intermediate states possess an ion core configuration of the first excited ionic state $^2D^o$ as indicated by the single prime. Although $^2D^o$ ions are the only ones allowed according to the conventional ionization rules, preserving the ion core may be an additional driving force for their formation.

(2) $(^2D^o)4p'\,^3D_J$. In this case, the ionization selection rules allow both $^2D^o$ and $^2P^o$ ions to be formed, however, we observe only $^2D^o$ ions. Although one could argue that our spectrometer may discriminate against low energy electrons from formation of $^2P^o$ ions, we do detect electrons at energies as low as 0.54 eV at 255.150 nm and 1.16 eV electrons at 256.769 nm. Ion formation through these resonant states appears to be governed by ion core preservation.

(3) $(^2D^o)4p'\,^3P_J$. In this case, two of the three allowed ion states are observed. Again, we observe the predominant ionic state to be the one corresponding to the ion core of the intermediate state of the atom.

(4) $(^4S^o)6p\,^3P_J$. The trend in this data set is a propensity to preserve the ionic core by forming $^4S^o_{3/2}$ ions. However, it is not clear why the ion-core preservation is not adhered to as strongly as in cases involving $^2D^o$ ionic states. The $6p\,^3P_2 \leftarrow\leftarrow {}^3P_2$ transition at 256.769 nm yields our only example of formation of $S^+\,^2P^o$ via 2+1 REMPI.

State selection for production of sulfur ions has been observed previously[10] using H_2S precursor molecules. In the wavelength range 288–311 nm, Steadman and Baer[10] documented core-preserving 2+1 REMPI transitions which produce pure populations of $^4S^o$ and $^2D^o$ S^+ ions. They reported other transitions with branching ratios that reflect ion-core preservation. This is also the general trend of our results. For example, state-selected $^2D^o$ sulfur ions can be produced efficiently using 2+1 REMPI via the $4p'\,^3D_J$ and $4p'\,^3F_J$ resonant levels. This state selection follows from the weak coupling of the Rydberg electron to the ion core of the excited sulfur atoms. This effect has been demonstrated[12] for transition metal atoms, as well,

TABLE III. Fitted photoelectron angular distribution coefficients for (2+1) REMPI of atomic sulfur produced via photodissociation of SO_2.

Ground state	Intermediate state	Ionic state	Wavelength (nm)	A_2[a]	A_4[b]
$^3P_0$	$4p'\,^3P_0$	$^4S^o$	253.662	1.36	−0.01
		$^2D^o$		0.88	0.08
	$4p'\,^3D_{2,1}$	$^2D^o$	257.801	0.73	−0.87[c]
	$4p'\,^3F_2$	$^2D^o$	256.950	1.90	0.78
	$6p\,^3P_0$	$^4S^o$	258.649	0.94	0.07
		$^2D^o$		0.43	0.07
	$6p\,^3P_2$	$^4S^o$	258.685	1.78	0.92
		$^2D^o$		0.60	−0.16
$^3P_1$	$4p'\,^3P_1$	$^4S^o$	253.132	0.57	0.07
		$^2D^o$		0.61	−0.03
	$4p'\,^3D_{2,1}$	$^2D^o$	257.214	1.01	−0.35
	$4p'\,^3D_3$	$^2D^o$	257.056	0.38	−0.71[c]
	$4p'\,^3F_2$	$^2D^o$	256.364	1.63	0.49
	$4p'\,^3F_3$	$^2D^o$	256.278	2.10	0.93
	$6p\,^3P_1$	$^2D^o$	258.004	1.01	0.38
	$6p\,^3P_2$	$^2D^o$	258.094	0.63	−0.09
$^3P_2$	$4p'\,^3D_{2,1}$	$^2D^o$	255.908	1.72	0.33
	$4p'\,^3D_3$	$^2D^o$	255.744	1.24	−0.31
	$4p'\,^3F_2$	$^2D^o$	255.069	1.46	−0.23
	$4p'\,^3F_3$	$^2D^o$	254.980	1.82	0.29
	$4p'\,^3F_4$	$^2D^o$	254.893	1.92	0.71
	$6p\,^3P_0$	$^4S^o$	256.741	1.42	0.15
		$^2D^o$		0.55	0.14
	$6p\,^3P_2$	$^4S^o$	256.769	0.81	−0.82[c]
		$^2D^o$		0.35	−0.01
$^1D_2$	$5p\,^1P_1$[d]	$^4S^o$	255.150	0.37	0.03

[a]Estimated error of ±0.10 (see the text).
[b]Estimated error of ±0.15 (see the text).
[c]These angular distributions are peaked at 45°.
[d]Two-photon autoionization, not 2+1 REMPI (Ref. 26).

and depends on the absence of perturbations from nearby neutral states or interaction with autoionizing levels in the continuum. The energy level structure of sulfur makes it particularly amenable to these types of excitations.

D. Photoelectron angular distributions

The most notable conclusions can be made regarding 2+1 ionizations of the ground state $^3P_0$ sulfur atoms, because these result from excitations of symmetric (unaligned) initial states. Thus any intermediate state alignment is due solely to the optical process. Photoelectrons ejected during ionization of symmetric intermediate states ($J \leqslant \frac{1}{2}$) must have a $P_2(\cos\Theta)$ distribution. In the case of resonant states with $J'=0$, k_{max} is restricted by the relation $J+1=1$. Contributions from high l partial waves are thus masked by the isotropic nature of the intermediate level

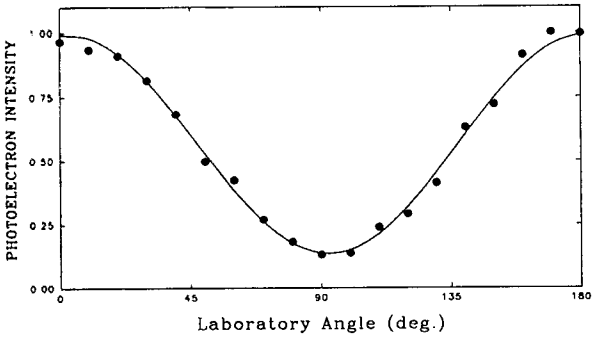

FIG. 5. Normalized photoelectron angular distributions for 2+1 REMPI via the $4p'\,^3P_0 \leftarrow\leftarrow {}^3P_0$ transition to form $^4S^o$ ground state sulfur ions. The solid line fits the data points best with $A_2=1.36$. Within the error of the fit, higher-order Legendre coefficients are equal to zero.

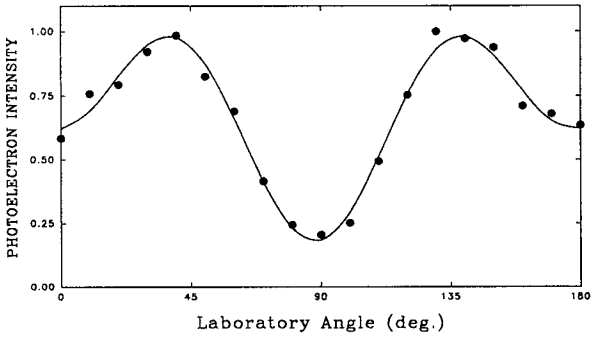

FIG. 6. Normalized photoelectron angular distributions for 2+1 REMPI via the $6p\,^3P_2 \leftarrow\leftarrow {}^3P_2$ transition to form $^4S^o$ ground state sulfur ions. The solid line fits the data points best with Legendre coefficients $A_2=0.81$ and $A_4=-0.82$.

structure. Previous 2+1 REMPI-PES of carbon[28] and nitrogen[29] atoms showed A_2 coefficients of 0.6 and -0.2 for ionization of symmetric $C\ 3p\ ^1S_0$ and $N\ 3p\ ^2S^o_{1/2}$ levels, respectively. The $4p'\ ^3P_0$ and $6p\ ^3P_0$ intermediate states accessed in our experiments are also symmetric and yield photoelectron angular distributions fit by the $P_2(\cos\Theta)$ term only (Table III).

REMPI of $^3P_0$ ground state sulfur atoms through resonant levels with $J'>0$ result in photoelectron angular distributions which are best fit using both $P_2(\cos\Theta)$ and $P_4(\cos\Theta)$ Legendre terms. States such as $6p\ ^3P_2$ can be highly aligned in the two-photon absorption process originating from the $^3P_0$ ground state. These higher-order fits reflect this optical alignment. As stated previously, the 2+1 REMPI process can yield aligned states fit to a Legendre expansion with $k=3$ ($k_{\max}=n+1$). However, no fits in our study required the $P_6(\cos\Theta)$ term. This follows from the selection rule for ionization of the $4p'$ and $6p$ intermediate states, namely $\Delta l=\pm 1$, which yields $l_e=0,2$. In fact, the resultant anisotropic angular distributions reflect competition between these two outgoing channels.[30] We expect the character of the outgoing electrons to be a mixture of s and d partial waves, with $l_{\max}$ then equal to 2, yielding Legendre fits restricted to A_2 and A_4 coefficients only ($k_{\max}=l_{\max}=2$). The fits in Table III for ionization of $^3P_0$ sulfur atoms through resonant states with $J'>0$ are consistent with this expectation.

The data presented in Table III for ionization of $^3P_0$ sulfur atoms show some characteristics which are repeated for other REMPI transitions. For instance, we measured angular distributions of electrons resulting from six transitions which lead to formation of both ground state ($^4S^o$) and excited state ($^2D^o$)S^+ ions. In general, angular distribution data from formation of $^4S^o$ ions were fit with larger A_2 and A_4 coefficients. Three cases investigated involve 2+1 ionization of resonant $^3P_0$ excited states, which closely parallel single-photon ionizations with photoelectron angular distributions fitted with the single asymmetry parameter β. Differences in the value of A_2 coefficients for processes which yield different ionic states is consistent with predicted deviations from the Cooper–Zare formalism.[31] Using $3p^4\ ^3P$ sulfur atoms as an example, Dill, Starace, and Manson[32] calculated significant influence of anisotropic electron–ion interactions on the form of photoelectron angular distributions from single-photon ionization of open-shell atoms.

During multiphoton ionization, the overall anisotropy of the resultant ion and electron is imparted by the summed absorption of each photon. The photoelectron angular distribution and alignment of the cation must carry away this anisotropy. In previous REMPI experiments with vanadium[33] it was shown that cation states of high J are able to accommodate more of this anisotropy than low J states. We are unable to discriminate between any J state preferences due to the closeness in energy for formation of $^2D^o_{3/2}$ and $^2D^o_{5/2}$ ionic states. We do observe, however, that photoelectron angular distributions from creation of $^4S^o_{3/2}$ ions are more anisotropic than those for formation of the $^2D^o_J$ states. Smaller coefficients for fits to $^2D^o$ production may reflect the ability of this excited ionic state to preferentially "remove" anisotropy from the system. Five of the six observed transitions of this type follow this trend.

The fit for the 2+1 REMPI $4p'\ ^3D_{2,1}\leftarrow\leftarrow{}^3P_0$ transition is peaked at 45° instead of the more common 0°. This anomaly is repeated twice more in Table III and is shown graphically in Fig. 6 for the case of $6p\ ^3P_2\leftarrow\leftarrow{}^3P_2$. Fits of this type are characterized by a relatively low A_2 coefficient and a relatively large, negative A_4 coefficient. The three cases observed in our experiments do not seem to have any obvious connection, but they are unique from a geometric point of view. The maximum intensity of photoelectrons from these ionizations is observed when the polarization vector of the laser is canted at a 45° angle with respect to the time-of-flight axis. This seems to be a rare observation for photoelectron angular distributions in REMPI of atoms.

The $^3P_1$ and $^3P_2$ sulfur atoms examined in this study can be aligned in the process of their formation from photodissociation of parent SO_2 molecules. Therefore the initial M_J state distributions for these atoms may be biased and additional optical absorption will yield a complex intermediate state. One-color ionization of these states will yield photoelectron angular distributions that cannot be deconvoluted to assess contributions from initial state alignments. It is our hope that future work using a two-color approach such as circularly dichroic angular distributions (CDAD)[34,35] or polarization-into-detector angular distributions (PINDAD)[36] will allow analysis of initial state alignments produced by the photodissociation event.

In the absence of our ability to remove contributions of initial state anisotropy to intermediate state alignment, only modest assessment of most photoelectron angular distributions reported in Table III can be made. In general, analytical fits require both $P_2(\cos\Theta)$ and $P_4(\cos\Theta)$ Legendre terms, which implies a contribution from partial waves with d character. Since no higher-order terms are revealed from the fit, we may assume that the description of complex alignment in the intermediate states is restricted by the $l_{\max}=2$ limit. All resonant states have p character and could yield distributions fit by A_2 and A_4 coefficients as long as $J'>0$. A few such states are fit with A_2 only, implying that they may not be highly aligned, or that interference of s and d partial waves reduces the observable alignment.

One transition of sulfur atoms created in an excited initial state ($^1D_2$) was observed. This two-photon autoionization via the $5p\ ^1P_1$ autoionizing level yielded a photoelectron angular distribution fit with the $P_2(\cos\Theta)$ Legendre term only. The A_2 coefficient thus obtained is similar to the β asymmetry parameter which could be extracted using a one-photon ionization. The resulting A_2 coefficient for this autoionization is one of the lowest values determined for any of the observed photoelectron angular distributions.

V. CONCLUSIONS

We have observed 2+1 REMPI of sulfur atoms borne from two-photon dissociation of parent SO_2 molecules in

the UV region between 252 and 263 nm. The sharp resonances correspond to excitation almost exclusively from ground state sulfur atoms. Initial and final states have been determined through analysis of the REMPI-PES. The four intercombination lines observed in this wavelength range were highly dependent on the energy of the laser. We verify a previous suggestion[10,37] that configuration interaction among the $6p\ ^5P_1$, $6p\ ^3P_1$, and $4p'\ ^1P_1$ excited states leads to intercombination transitions in the two-photon absorption.

State selection of $S^+(^2D^o)$—and to a lesser extent $S^+(^4S^o)$—has been demonstrated at many wavelengths, indicating a propensity toward ion-core preservation in the ionization process. Therefore this method can be used to produce ions in selected states for use as possible precursors in ion–molecule reactions.

Photoelectron angular distributions revealed contributions of outgoing continuum electrons with high l components ($l_{max}=2$). REMPI transitions which originated from the $^3P_0$ ground state of sulfur show optical alignment in intermediate states with $J'>0$. It is hoped that future two-color CDAD or PINDAD experiments using ground state sulfur atoms with $J''>0$ will afford a description of initial state alignment caused by the photodissociation event. A comparison of different parent molecules (SO_2, OCS, CS_2, e.g.) which yield the same types of aligned atoms might provide interesting information about the dissociation event.

ACKNOWLEDGMENTS

The authors wish to thank the American Philosophical Society for partial support of this project. J.R.A. and A.C.G. acknowledge the Donors of the Petroleum Research Fund, administered by the American Chemical Society. Additional support for A.C.G. was also provided by Kentucky EPSCoR. Partial support for M.R.H. was provided by the University of Kentucky Institute for Mining and Minerals Research. Support for R.A.E. was provided by the NSF Research Experiences for Undergraduates program. The photoion/photoelectron spectrometer system was constructed using funds from the University of Kentucky Major Research Instrumentation Bond Program (item ID# 7E-8E56-23).

[1] J. M. Wallace and P. V. Hobbs, *Atmospheric Science, An Introductory Survey* (Academic, New York, 1977).
[2] C. S. Effenhauser, P. Felder, and J. R. Huber, Chem. Phys. **142**, 311 (1990).
[3] T. Venkitachalam and R. Bersohn, J. Photochem. **26**, 65 (1984).
[4] C. Lalo and C. Vermeil, J. Photochem. **3**, 441 (1974/75).
[5] T. V. Venkitachalam and A. S. Rao, Appl. Phys. B **52**, 102 (1991).
[6] P. Brewer, N. Van Veen, and R. Bersohn, Chem. Phys. Lett. **91**, 126 (1982).
[7] G. Black and L. E. Jusinski, Chem. Phys. Lett. **124**, 90 (1986).
[8] S. T. Pratt, Phys. Rev. A **38**, 1270 (1988).
[9] N. Sivakumar, G. E. Hall, and P. L. Houston, J. Chem. Phys. **88**, 3692 (1988).
[10] J. Steadman and T. Baer, J. Chem. Phys. **89**, 5507 (1988).
[11] C. E. Moore, *Atomic Energy Levels* (Natl. Stand. Ref. Data Ser., Natl. Bur. Standard. Cir. 35, U.S. Government Printing Office, Washington, D.C., 1971), Vol. 1; W. C. Martin, R. Zalubas, and A. Musgrove, J. Phys. Chem. Ref. Data **19**, 820 (1990).
[12] L. Sanders, A. D. Sappey, and J. C. Weisshaar, J. Chem. Phys. **85**, 6952 (1986).
[13] L. Sanders, S. D. Hanton, and J. C. Weisshaar, J. Chem. Phys. **92**, 3498 (1990).
[14] P. Lambropoulos, Adv. At. Mol. Phys. **12**, 87 (1976).
[15] M. P. Strand, J. Hansen, R.-L. Chien, and R. S. Berry, Chem. Phys. Lett. **59**, 205 (1978).
[16] S. N. Dixit and P. L. Lambropoulos, Phys. Rev. Lett. **46**, 1278 (1978); Phys. Rev. A **27**, 168 (1983).
[17] S. N. Dixit and V. McKoy, J. Chem. Phys. **82**, 3546 (1985).
[18] J. R. Appling, M. G. White, W. J. Kessler, R. Fernandez, and E. D. Poliakoff, J. Chem. Phys. **88**, 2300 (1988).
[19] J. Cooper and R. N. Zare, J. Chem. Phys. **48**, 942 (1968).
[20] J. L. Dehmer, D. Dill, and A. C. Parr, in *Photophysics and Photochemistry in the Vacuum Ultraviolet*, edited by S. McGlynn, G. Findley, and R. Huebner (Reidel, Dordrecht, 1985), p. 341.
[21] T. A. Carlson, M. O. Krause, J. W. Taylor, P. R. Keller, M. N. Piancastelli, F. A. Grimm, and T. A. Whitley, IEEE Trans. Nucl. Sci. **30**, 1034 (1983).
[22] P. J. Miller, W. A. Chupka, J. Winniczek, and M. G. White, J. Chem. Phys. **89**, 4058 (1988).
[23] M. Asscher, W. L. Guthrie, T. H. Lin, N. Ohmichi, J. Silberstein, and R. D. Levine, Laser Chem. **5**, 239 (1985).
[24] R. N. Compton and J. C. Miller, *Laser Applications in Physical Chemistry*, edited by D. K. Evans (Marcel Dekker, New York, 1989).
[25] C. H. Greene and R. N. Zare, Annu. Rev. Phys. Chem. **33**, 119 (1982).
[26] J. R. Appling, M. R. Harbol, R. A. Edgington, A. C. Goren, and S. Lai, Chem. Phys. Lett. **184**, 428 (1991).
[27] L. R. Jakobsson, Ark. Fys. **34**, 19 (1967).
[28] S. T. Pratt, J. L. Dehmer, and P. M. Dehmer, J. Chem. Phys. **82**, 676 (1985).
[29] S. T. Pratt, J. L. Dehmer, and P. M. Dehmer, Phys. Rev. A **36**, 1702 (1987).
[30] J. Cooper and R. N. Zare, J. Chem. Phys. **48**, 942 (1968).
[31] J. Cooper and R. N. Zare, *Lectures in Theoretical Physics*, edited by S. Geltman, K. T. Mahanthappa, and W. E. Britten (Gordon and Breach, New York, 1969), Vol. XI-C, 317–337.
[32] D. Dill, A. F. Starace, and S. T. Manson, Phys. Rev. A **11**, 1596 (1975).
[33] L. Sanders, S. D. Hanton, and J. C. Weisshaar, J. Chem. Phys. **92**, 3485 (1990).
[34] R. L. Dubs, S. N. Dixit, and V. McKoy, J. Chem. Phys. **85**, 656 (1986).
[35] J. R. Appling, M. G. White, R. L. Dubs, S. N. Dixit, and V. McKoy, J. Chem. Phys. **87**, 6927 (1987).
[36] R. L. Dubs, V. McKoy, and S. N. Dixit, J. Chem. Phys. **88**, 968 (1988).
[37] J. F. Alder, R. M. Bombelka, and G. F. Kirkbright, J. Phys. B **11**, 235 (1978).